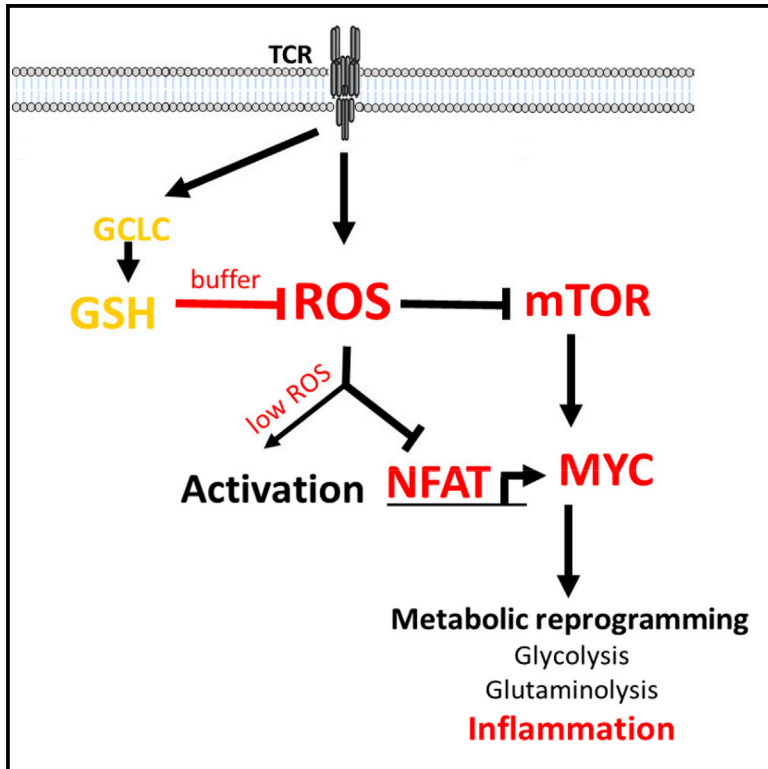# Glutathione Primes T Cell Metabolism for Inflammation

Graphical Abstract

Authors

Tak W. Mak, Melanie Grusdat,
Gordon S. Duncan, ..., Isaac S. Harris,
Karsten Hiller, Dirk Brenner

Correspondence

tmak@uhnresearch.ca (T.W.M.),
dirk.brenner@lih.lu (D.B.)

In Brief

Upon activation, T cells adapt their metabolism to meet their increased bioenergetic and biosynthetic needs. Activated T cells produce ROS, which trigger the antioxidative GSH response to prevent cellular damage. Mak et al. report that the GSH pathway plays an unexpected role in metabolic integration during inflammatory T cell responses.

Highlights

- Glutathione (GSH) is not needed for early T cell activation but promotes T cell growth

- GSH supports mTOR and NFAT activity and drives glycolysis and glutaminolysis

- Gclc-derived GSH buffers ROS and regulates Myc-dependent metabolic reprogramming

- Ablation of Gclc in T cells impairs inflammatory responses in vivo

CellPress

Glutathione Primes
T Cell Metabolism for Inflammation

Tak W. Mak,[1,2,16,*] Melanie Grusdat,[3,16] Gordon S. Duncan,[1] Catherine Dostert,[3] Yannic Nonnenmacher,[4,5] Maureen Cox,[1] Carole Binsfeld,[3] Zhenyue Hao,[1,6] Anne Brüstle,[7] Momoe Itsumi,[8] Christian Jäger,[5] Ying Chen,[9] Olaf Pinkenburg,[10] Bärbel Camara,[10] Markus Ollert,[11,12] Carsten Bindslev-Jensen,[12] Vasilis Vasiliou,[9] Chiara Gorrini,[1] Philipp A. Lang,[13] Michael Lohoff,[10] Isaac S. Harris,[14] Karsten Hiller,[4,5,15] and Dirk Brenner[3,12,17,*]

[1]The Campbell Family Cancer Research Institute and University Health Network, Toronto, ON M5G 2C1, Canada
[2]Departments of Medical Biophysics and Immunology, University of Toronto, Toronto, ON M5G 2M9, Canada
[3]Department of Infection and Immunity, Experimental and Molecular Immunology, Luxembourg Institute of Health, Esch-sur-Alzette, L-4354, Luxembourg
[4]Technische Universität Braunschweig, Braunschweig Integrated Center of Systems Biology, Braunschweig D-38106, Germany
[5]Luxembourg Centre for Systems Biomedicine, University of Luxembourg, Belvaux, L-4367, Luxembourg
[6]The Donnelly Centre for Cellular and Biomolecular Research, University of Toronto, Toronto, ON M5S3E1 Canada
[7]Department of Immunology and Infectious Disease, John Curtin School of Medical Research, Australian National University, Canberra, ACT 2601, Australia
[8]Department of Molecular Virology, Tokyo Medical and Dental University, Tokyo, 113-8510, Japan
[9]Department of Environmental Health Sciences, Yale School of Public Health, CT 06520, New Haven, USA
[10]Institute for Medical Microbiology and Hospital Hygiene, University of Marburg, Marburg, D-35032 Germany
[11]Department of Infection and Immunity, Allergy and Clinical Immunology, Luxembourg Institute of Health, Esch-sur-Alzette, L-4354, Luxembourg
[12]Odense Research Center for Anaphylaxis, Department of Dermatology and Allergy Center, Odense University Hospital, University of Southern Denmark, Odense, DK-5000, Denmark
[13]Department of Molecular Medicine II, Medical Faculty, University of Düsseldorf, Düsseldorf, D-40225, Germany
[14]Department of Cell Biology, Harvard Medical School, Boston, MA 02115, USA
[15]Computational Biology of Infection Research, Helmholtz Centre for Infection Research, Braunschweig, D-38124, Germany
[16]These authors contributed equally to this work
[17]Lead contact
*Correspondence: tmak@uhnresearch.ca (T.W.M.), dirk.brenner@lih.lu (D.B.)
http://dx.doi.org/10.1016/j.immuni.2017.03.019

SUMMARY

Activated T cells produce reactive oxygen species (ROS), which trigger the antioxidative glutathione (GSH) response necessary to buffer rising ROS and prevent cellular damage. We report that GSH is essential for T cell effector functions through its regulation of metabolic activity. Conditional gene targeting of the catalytic subunit of glutamate cysteine ligase (*Gclc*) blocked GSH production specifically in murine T cells. Gclc-deficient T cells initially underwent normal activation but could not meet their increased energy and biosynthetic requirements. GSH deficiency compromised the activation of mammalian target of rapamycin-1 (mTOR) and expression of NFAT and Myc transcription factors, abrogating the energy utilization and Myc-dependent metabolic reprogramming that allows activated T cells to switch to glycolysis and glutaminolysis. In vivo, T-cell-specific ablation of murine *Gclc* prevented autoimmune disease but blocked antiviral defense. The antioxidative GSH pathway thus plays an unexpected role in metabolic integration and reprogramming during inflammatory T cell responses.

INTRODUCTION

T cells are activated when their T cell receptors (TCRs) are engaged by cognate peptide-MHC complexes. TCR triggering initiates activation, proliferation, and differentiation associated with effector function acquisition. Coordinated activation of ERK, JNK, NFAT, and NF-κB signaling and responses to mitogens such as IL-2 are critical for T cell functionality (Brownlie and Zamoyska, 2013). Activated T cells undergo clonal expansion that dramatically raises their bioenergetic needs and requires increased glucose and glutamine utilization (Carr et al., 2010; Frauwirth et al., 2002; Pollizzi and Powell, 2014). This heightened metabolic activity drives increased production of reactive oxygen species (ROS) by the mitochondrial electron transport chain (Gülow et al., 2005; Sena et al., 2013; Yi et al., 2006). Whereas low concentrations of ROS support cell survival and proliferation, high concentrations of ROS initiate DNA damage and cell death (Cairns et al., 2011; Gorrini et al., 2013; Sena and Chandel, 2012). Activated T cells control their rising concentrations of ROS by using endogenous antioxidants, particularly glutathione (GSH) (Meister, 1983). The rate-limiting step in GSH synthesis is catalyzed by glutamate cysteine ligase (GCL), composed of catalytic (GCLC) and modifier (GCLM) subunits (Chen et al., 2005). Gene-targeting of *Gclc* in mice is embryonically lethal (Chen et al., 2007), precluding analysis of GSH functions in adult mice.

In this study, we analyzed conditional mutant mice lacking *Gclc* (and thus GSH) specifically in T cells, and we report that GSH is essential for the energy metabolism changes required for T cell effector functions. GSH-deficient T cells initially undergo normal activation but cannot reprogram their metabolism to meet their rising energy needs. As a result, autoimmune responses are prevented, and antiviral defenses are inhibited in vivo. Our data position the GSH pathway as a central metabolic integrator in inflammatory responses mediated by T cells.

RESULTS

GSH Is Dispensable for Early T Cell Activation but Promotes T Cell Growth

Because proliferating T cells accumulate ROS (Devadas et al., 2002; Gülow et al., 2005; Jackson et al., 2004; Yi et al., 2006), we speculated that the GSH pathway might be upregulated in these cells. We activated naive wild-type (WT) murine T cells in vitro with anti-CD3 plus anti-CD28 antibodies (αCD3+αCD28) and measured *Gclc* and *Gclm* mRNAs by quantitative RT-PCR. *Gclc* mRNA, but not *Gclm* mRNA, was upregulated upon TCR triggering (Figure 1A). This *Gclc* upregulation was inhibited by the addition of buthionine sulfoximine (BSO), a specific inhibitor of GCL activity (Figure S1A in the Supplemental Information online), indicating that the GSH pathway is activated by TCR triggering. We then crossed Cd4cre-expressing mice with *Gclc*$^{fl/fl}$ mice to generate progeny (*Cd4cre-Gclc*$^{fl/fl}$ mice) in which *Gclc* was deleted specifically in T cells (Figure S1B). GSH was minimal in naive CD4$^+$ and CD8$^+$ T cells isolated from spleen and lymph nodes (LNs) of these mutants but increased sharply in these cells after activation with αCD3+αCD28 in vitro for 24 hr (Figure 1B) or when the mice had been injected with anti-CD3 or Staphylococcal enterotoxin B (SEB) so that T cells would be activated in vivo (Figure 1C and Figure S1C). *Cd4cre-Gclc*$^{fl/fl}$ mice showed normal thymocyte development but reduced peripheral CD8$^+$ and CD4$^+$ T cells (Figures S1E and S1F). Thus, *Gclc* is important for T cell homeostasis and GSH synthesis.

We expected that *Cd4cre-Gclc*$^{fl/fl}$ T cells would accumulate high concentrations of ROS, but DCF-DA staining and flow-cytometric examination of activated control and mutant CD4$^+$ and CD8$^+$ T cells showed that the concentrations of ROS were only modestly increased in Gclc-deficient T cells activated in vitro (Figure 1D) or in vivo (Figure 1E and Figure S1D). CD69 and CD44 expression were comparably induced on T cells of both genotypes in vivo (Figure 1F) and in vitro (Figure 1G), indicating that *Gclc* is not crucial for the initial stages of T cell activation. Accordingly, immunoblotting revealed similar activation kinetics of TCR-proximal signaling molecules in control and *Cd4cre-Gclc*$^{fl/fl}$ T cells, although p38, ERK and JNK phosphorylation were slightly greater in the mutant cells (Figures S2A and S2B). However, the ability of activated T cells to become large blasts was reduced by Gclc deficiency both in vitro (Figure 1H) and in vivo (Figure S2C), and cell death was increased upon 48 hr stimulation (Figure S2D). Thus, GSH is dispensable for initial T cell activation but governs T cell homeostasis in vivo and promotes activation-dependent growth.

T-Cell-Intrinsic *Gclc* Is Required for mTOR Activation

T cell blasts exhibit an increase in cell volume that is controlled by mammalian target of rapamycin complex-1 (mTORC1) (Laplante and Sabatini, 2012). We investigated whether Gclc deficiency reduced mTOR activity in CD4$^+$ and CD8$^+$ T cells stimulated with αCD3+αCD28 in vitro. Flow cytometry and immunoblotting confirmed that Gclc deficiency blocked mTOR S2448 phosphorylation as well as phosphorylation of the mTORC1 targets S6 and 4E-BP1 (Figures 2A–2C). Addition of the mTOR inhibitor rapamycin confirmed that the effect was mTOR specific. Cells control mTOR activity via inhibitory phosphorylation of tuberous sclerosis complex 2 (TSC2) by AKT or GSK3β (Inoki et al., 2006), but we found no differences in AKT or GSK3β activation between control and mutant T cells (Figure S2B). To test whether elevated ROS reduced mTOR activity in *Cd4cre-Gclc*$^{fl/fl}$ T cells, we stimulated T cells of both genotypes with αCD3+αCD28 and treated them with GSH or another antioxidant, N-acetyl-cysteine (NAC). The elevated concentrations of ROS in activated Gclc-deficient T cells were reduced to near-WT concentrations by NAC or GSH (Figure S2E). Both mTOR activation and S6, p70, and 4E-BP1 phosphorylation were partially restored (Figures 2D–2F), suggesting that these signaling alterations in Gclc-deficient T cells were largely due to a lack of ROS buffering.

Gclc Supports Glutamine Metabolism

mTOR responds to nutrient deficiency by stimulating the synthesis of proteins, nucleotides, and lipids (Laplante and Sabatini, 2012). We speculated that Gclc deficiency in T cells might inhibit mTOR activation and glutamine utilization. CD98 is a heterodimeric amino acid transporter that is induced in activated T cells and crucial for glutamine uptake (Nicklin et al., 2009). We found that activated Gclc-deficient T cells expressed less surface CD98 than controls (Figure 3A). We then measured glutamine anaplerosis into the TCA cycle by calculating the molar difference between glutamine uptake and glutamate secretion. The net influx of glutamine-derived carbon was decreased in activated mutant T cells compared to controls (Figure 3B). Next, we activated mutant and control T cells with αCD3+αCD28 in the presence of U-^{13}C-glutamine and determined its incorporation into downstream metabolites by analyzing mass isotopomer distributions (MIDs) of TCA cycle intermediates under metabolic and isotopic steady-state conditions (Figure 3C, left). Although the relative flux of glutamine into TCA intermediates in activated T cells of both genotypes was higher than steady-state values, this increase was less in Gclc-deficient T cells (Figure 3C). Citrate M4 mass isotopomers indicate oxidative TCA metabolism of glutamine. A subsequent cycle generates M2 mass isotopomers (oxidative decarboxylation by isocitrate dehydrogenase and 2-oxoglutarate dehydrogenase). An increased ratio of M2 to M4 citrate isotopologues thus represents heightened TCA activity (Figure S3A). The ratio of M2 to M4 citrate in activated mutant T cells was higher than that in controls (Figure S3B), suggesting an increase in overall TCA flux in the absence of GSH. However, because glutamine anaplerosis is decreased in Gclc-deficient T cells, this increased TCA activity must be driven by another carbon source.

Because glutamine is essential for T cell proliferation (Carr et al., 2010; Hörig et al., 1993; Newsholme et al., 1985; Yaqoob and Calder, 1997), we compared the proliferative capacities of activated *Cd4cre-Gclc*$^{fl/fl}$ and control T cells. The mutant T cells showed a striking lack of growth upon αCD3+αCD28
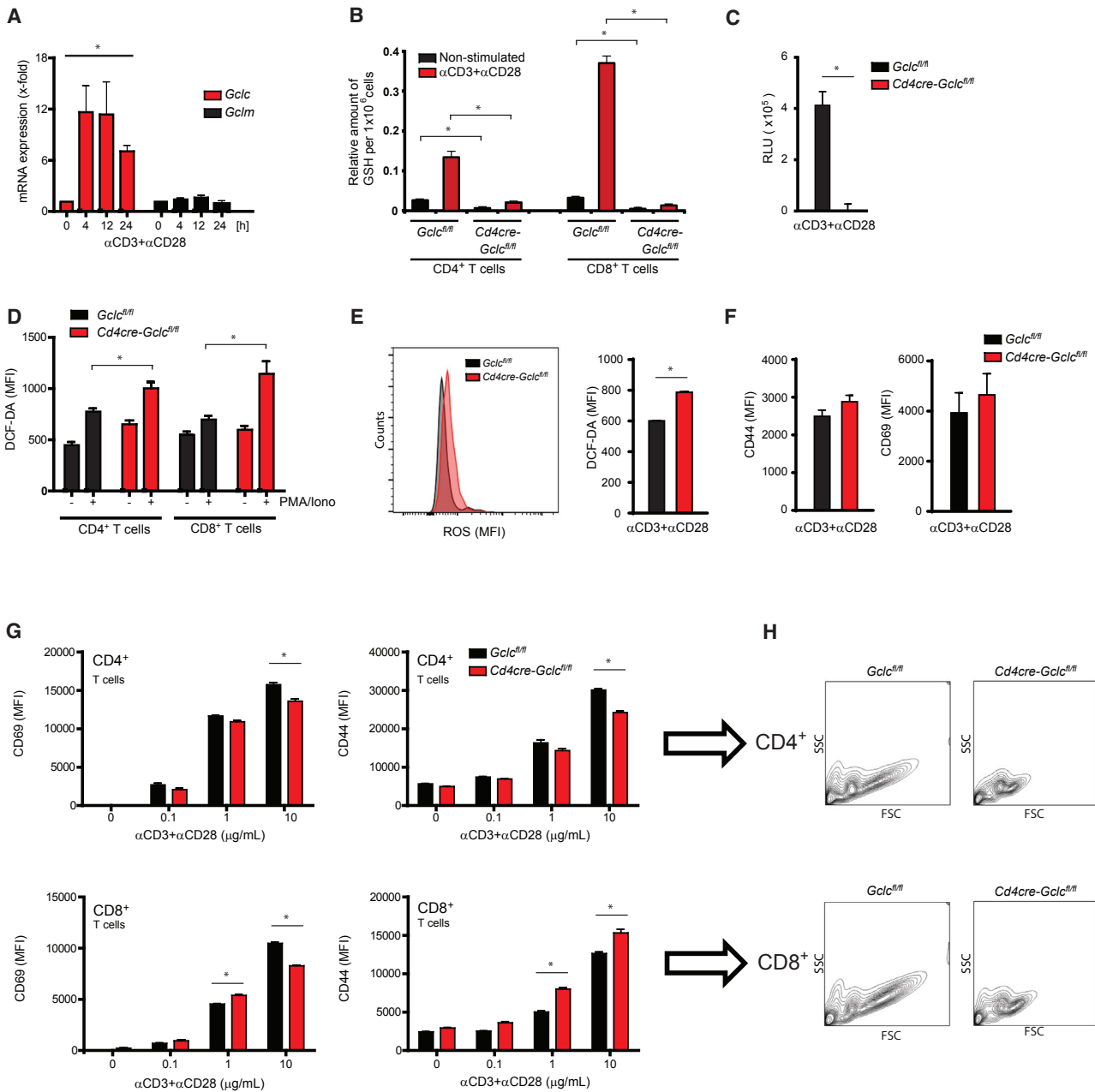
Figure 1. Gclc Deficiency Increases ROS Concentration in T Cells

(A) Quantitative RT-PCR analysis of *Gclc* and *Gclm* mRNAs in CD4+ T cells that were isolated from spleen and LN of WT mice and stimulated with αCD3+αCD28 for the indicated times. Data are means ± SEM (n = 3) and representative of two independent trials. *p < 0.05.

(B) LC-MS determination of GSH in *Gclc*^fl/fl^ and *Cd4cre-Gclc*^fl/fl^ CD4+ and CD8+ T cells that were stimulated with αCD3+αCD28 for 24 hr. Results are expressed as relative amounts of GSH per 1 × 10^6 T cells. Data are means ± SD for CD4+ (n = 3) and CD8+ (n = 2) T cells and representative of two independent trials.

(C) Determination of GSH in splenic and LN T cells isolated from *Gclc*^fl/fl^ and *Cd4cre-Gclc*^fl/fl^ mice 24 hr after i.p. injection with anti-CD3. Data are means ± SEM (n = 3) and representative of two independent trials.

(D) Flow-cytometric determination of ROS in *Gclc*^fl/fl^ and *Cd4cre-Gclc*^fl/fl^ CD4+ and CD8+ T cells that were stimulated with PMA and ionomycin for 24 hr and stained with DCF-DA. Data are means ± SEM (n = 3) and representative of three independent trials.

(E) Flow-cytometric determination of ROS in splenic and LN CD4+ T cells that were isolated from *Gclc*^fl/fl^ and *Cd4cre-Gclc*^fl/fl^ mice at 24 hr after injection with anti-CD3, followed by DCF-DA staining. Data are means ± SEM (n = 3) and representative of two independent trials.

(F and G) Flow-cytometric determination of surface expression of CD69 and CD44 by T cells that were either (F) isolated from *Gclc*^fl/fl^ and *Cd4cre-Gclc*^fl/fl^ mice 24 hr after injection with anti-CD3 or (G) stimulated in vitro for 24 hr with the indicated concentrations of αCD3+αCD28. Data are means ± SEM (n = 6) and representative of two (F) or six (G) independent trials.

(H) Flow-cytometric FSC and SSC measurements of the cells in (G). Data are representative of six independent trials. See also Figures S1 and S2.
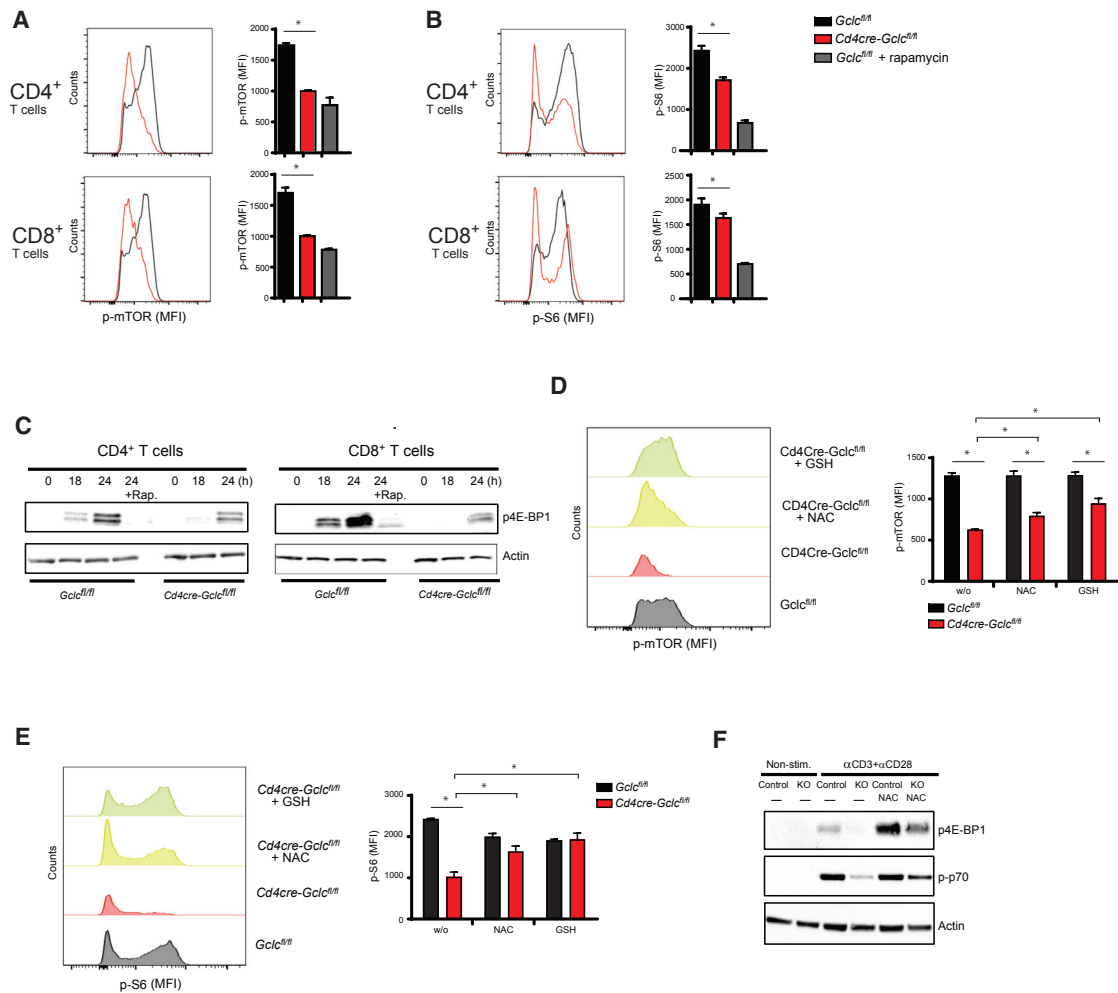
Figure 2. T-Cell-Intrinsic *Gclc* Drives mTOR Activation

(A and B) Intracellular flow-cytometric determination of phosphorylated mTOR (A) and phospho-S6 (B) in *Gclc^fl/fl* and *Cd4cre-Gclc^fl/fl* CD4^+ and CD8^+ T cells that were stimulated with αCD3+αCD28 ± rapamycin for 24 hr. Data are means ± SEM (n = 3) and representative of three independent trials.

(C) Immunoblot showing phospho-4EBP1 in *Gclc^fl/fl* and *Cd4cre-Gclc^fl/fl* CD4^+ and CD8^+ T cells that were stimulated for the indicated times with αCD3+αCD28 ± rapamycin. Loading control: actin. Data are representative of three independent trials.

(D and E) Intracellular flow-cytometric determination of p-mTOR (D) and p-S6 (E) in *Gclc^fl/fl* and *Cd4cre-Gclc^fl/fl* CD4^+ T cells that were stimulated with αCD3+αCD28 for 24 hr, with or without (w/o) NAC or GSH. Data are means ± SEM (n = 5) and representative of three independent trials.

(F) Immunoblot showing p-4EBP1 and p-p70 in *Gclc^fl/fl* (control) and *Cd4cre-Gclc^fl/fl* (KO) CD4^+ T cells that were stimulated with αCD3+αCD28 for 24 hr ± NAC. Data are representative of three independent trials.

stimulation, and this lack was not due to increased cell death (Figure 3D and Figure S3C). However, this proliferation deficit could not be rescued by excess glutamine or a cell-permeable α-ketoglutarate (αKG) derivative (dimethyl-αKG, DMK) (Figures S3D and S3E). Thus, Gclc deficiency not only impairs glutaminolysis but has other effects on T cells.

Gclc Regulates Metabolic Reprogramming

Proliferating T cells require fatty acids for lipid and membrane synthesis. These components are provided by increased glycolysis and glutaminolysis, which also fill the cellular energy pool with ATP (Frauwirth et al., 2002; Gerriets and Rathmell, 2012; Pearce and Pearce, 2013). To investigate whether Gclc loss

affected the energy pool, we measured ATP in activated control and mutant T cells. Intracellular ATP was decreased in resting mutant T cells compared to controls and did not increase upon activation (Figure 4A).

To determine whether *Gclc* regulates aerobic glycolysis, we applied a glycolysis stress test to mutant and control CD4^+ and CD8^+ T cells that had been activated in vivo with SEB for 48 hr prior to isolation, as well as to isolated T cells that had been activated in vitro with αCD3+αCD28 for 24 hr. Measurement of the extracellular acidification rate (ECAR) revealed that *Gclc* ablation reduced glycolysis in mutant T cells activated in vivo or in vitro (Figures 4B and 4C). Thus, GSH has an unexpected role in regulating glucose metabolism.
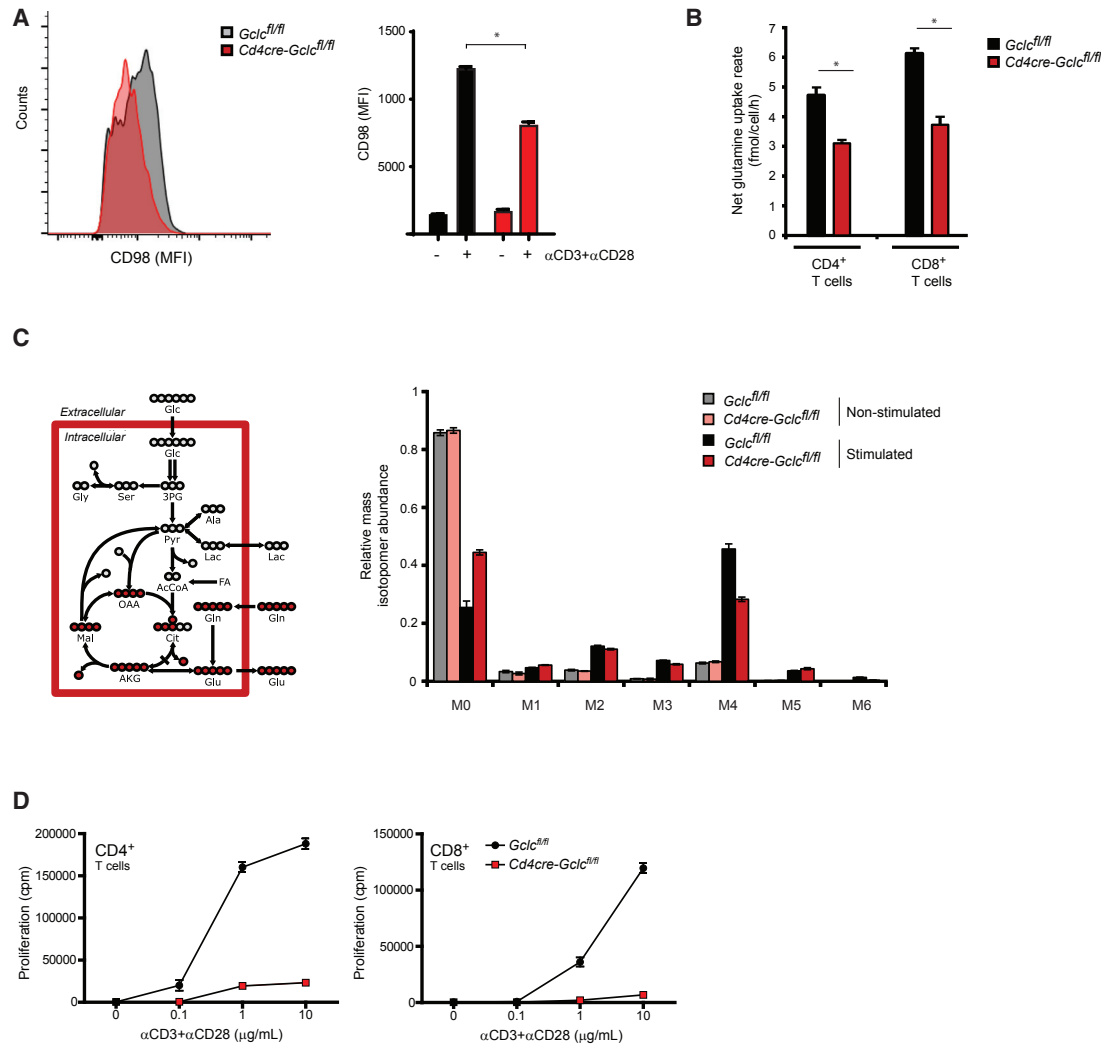
Figure 3. *Gclc* Is Required for Glutaminolysis in Activated T Cells

(A) Flow-cytometric determination of surface CD98 expression by *Gclc^fl/fl* and *Cd4cre-Gclc^fl/fl* CD4^+ T cells that were stimulated for 24 hr with αCD3+αCD28. Data on the right are means ± SEM (n = 3) and representative of three independent trials.

(B) Determination of glutamine anaplerosis in *Gclc^fl/fl* and *Cd4cre-Gclc^fl/fl* CD4^+ and CD8^+ cells that were stimulated for 24 hr with αCD3+αCD28. Data are means ± SEM (n = 3) and representative of three independent trials.
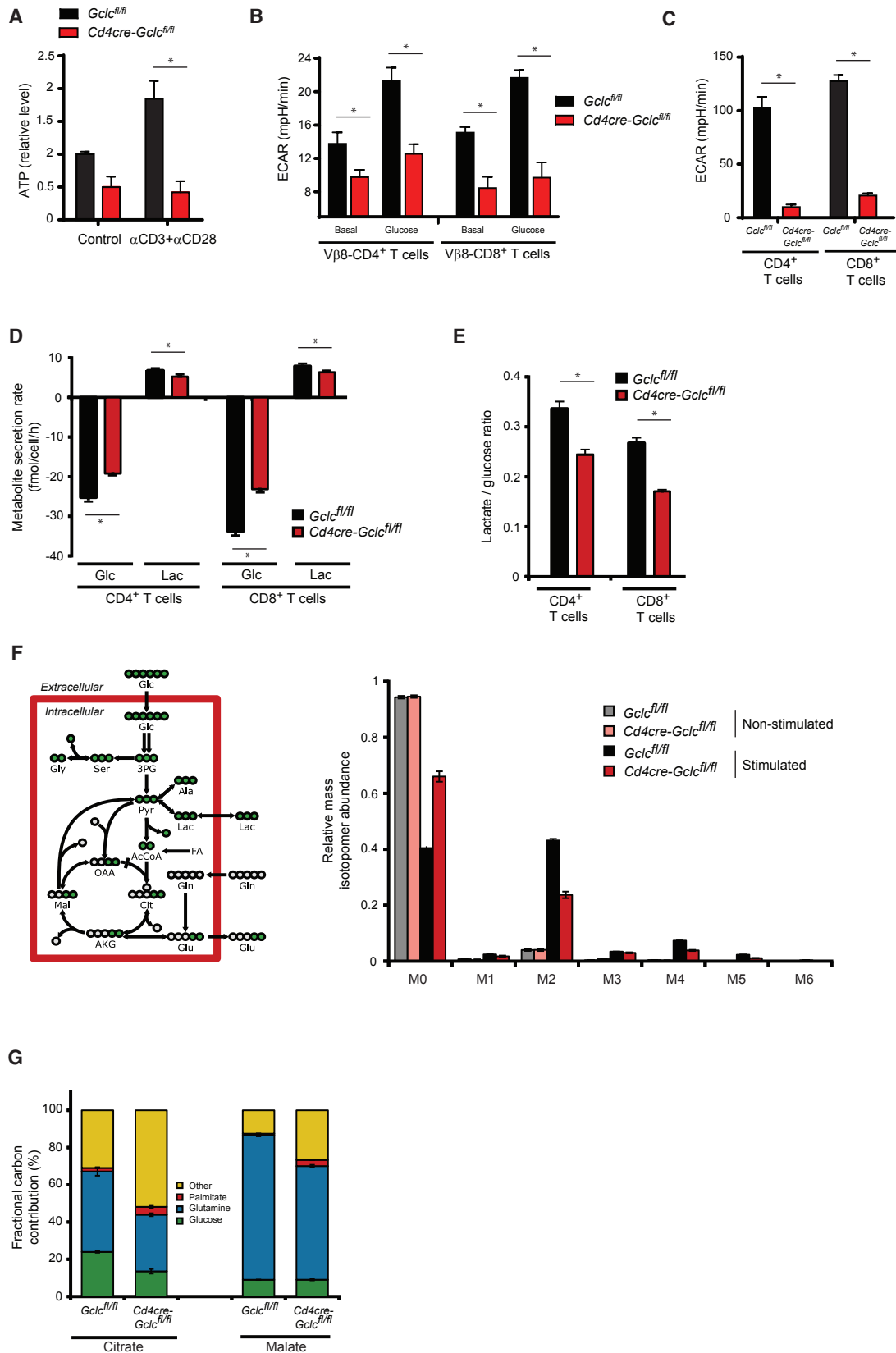
(C) Fluxmap of mammalian central carbon metabolism (left) and mass isotopomer distribution of citrate (right) for *Gclc^fl/fl* and *Cd4cre-Gclc^fl/fl* CD4^+ T cells that were incubated with U-^{13}C-glutamine and stimulated with αCD3+αCD28 for 24 hr. Data are means ± SEM (n = 3) and representative of three independent trials.

(D) Proliferation assessment by ^{3}H-thymidine incorporation of *Gclc^fl/fl* and *Cd4cre-Gclc^fl/fl* T cells that were stimulated with αCD3+αCD28 for 24 hr. Data are means ± SEM (n = 3) and representative of three independent trials. See also Figure S3.

We next measured glucose consumption and lactate secretion by Gclc-deficient and control T cells activated with αCD3+αCD28 over 24 hr. Mutant T cells consumed less glucose and produced less lactate than controls (Figure 4D), and the ratio of secreted lactate to consumed glucose (a measure of glycolytic ATP production) was decreased (Figure 4E). Thus, Gclc deficiency reduced the flux of glycolysis-derived pyruvate through lactate dehydrogenase (LDH) over the 24 hr activation period, indicating an altered glucose flux through pyruvate dehydrogenase (PDH) into the TCA cycle. When resting control and *Cd4cre-Gclc^fl/fl* T cells were incubated with U-^{13}C-glucose, equivalent fractions of M2 isotopologues of citrate, which represent the relative flux of glucose-derived carbon through PDH,

were observed (Figure 4F). Upon activation, flux through PDH increased strongly in T cells of both genotypes, but reduced M2 citrate isotopologues were found in *Cd4cre-Gclc^fl/fl* T cells, indicating decreased PDH activity. In contrast to M2 citrate, there was no decrease in TCA cycle-derived M1 citrate isotopologues in the absence of *Gclc*. M1 citrate is produced by subsequent cycling of M2 citrate, and the M1:M2 citrate ratio indicates TCA cycling activity (Figure S3F). Thus, overall TCA cycle activity was increased in the mutant T cells despite their GSH deficit, in line with our glutamine tracing experiments (Figure 3C and Figure S3B).

Although the relative contributions of glucose and glutamine carbons to the TCA cycle were decreased in the absence of

(legend on next page)

GSH, the overall activity of the cycle was increased. This result can only be explained by constant replenishment of the mitochondrial acetyl-CoA pool by another carbon source. To test whether this source was increased fatty-acid oxidation, we incubated mutant and control CD4$^+$ T cells with U-^{13}C-palmitate, which is transported into mitochondria and oxidized to yield acetyl-CoA. Indeed, fatty-acid β-oxidation was increased in Gclc-deficient T cells compared to controls (Figure 4G). However, there was still a large contribution to TCA cycle intermediates by carbon sources other than glutamine, glucose, and palmitate, and this contribution was greater in *Cd4cre-Gclc^fl/fl* T cells than in controls. Such sources might be fatty acids (including palmitate) derived from FBS in the culture medium or generated by the catabolism of branched-chain amino acids. During metabolic reprogramming of activated T cells, mitochondrial oxidative phosphorylation is increased (Chang et al., 2013). However, in accordance with their reduced ATP, the oxygen consumption rate (OCR) in activated Gclc-deficient T cells lower than that in controls (Figure S3G). Thus, the unknown additional carbon sources cannot compensate for the energy gap in Gclc-deficient T cells. GSH is therefore critical for metabolic reprogramming during T cell activation.

Ablation of Gclc Impairs TCR-Induced Myc Expression and NFAT Activation

The transcription factor Myc is involved in activation-induced glycolysis and glutaminolysis in T cells (Douglas et al., 2001; Verbist et al., 2016; Wang et al., 2011). To determine the role of *Gclc* in Myc expression, we activated control and mutant T cells with αCD3+αCD28 and visualized Myc protein by immunoblotting. Gclc deficiency reduced TCR-driven Myc upregulation (Figure 5A), revealing an unanticipated function for GSH in the Myc-regulated switch of T cell metabolism to glycolysis. To mimic Gclc deficiency in WT T cells, we treated them with BSO. Activated BSO-treated WT T cells showed reduced GSH after 24 hr and accumulated higher ROS than untreated WT T cells (Figure S4A and S4B). BSO-treated WT T cells also showed decreased Myc that was restored by NAC co-incubation (Figure 5B) and ROS scavenging (Figure S4C). Myc controls the alternative-splicing-mediated shift from pyruvate kinase (PKM) 1 to PKM2 expression (David et al., 2010) and facilitates glycolytic lactate production (Wang et al., 2011). Indeed, PKM2 protein was downregulated in *Cd4cre-Gclc^fl/fl* T cells (Figure S4D), in line with the altered glucose flux through PDH and reduced lactate production in these cells.

Next, we sought to determine which pathway mediates GSH-dependent Myc expression in T cells. Although NFAT can promote Myc production in cancer cells (Buchholz et al., 2006; Köenig et al., 2010; Singh et al., 2010), the situation in T cells is unclear. NFAT also drives mTOR expression, and mTOR stabilizes Myc translation (Babcock et al., 2013; Düvel et al., 2010; Hosoi et al., 1998). We stimulated WT T cells with αCD3+αCD28 plus the calcineurin inhibitor FK506 (which impairs NFAT activation) or rapamycin. Immunoblotting showed that inhibition of either NFAT or mTOR reduced Myc protein (Figure 5C) and that S6 phosphorylation was inhibited by FK506 (Figure 5C). Thus, NFAT controls mTOR activity and Myc production in T cells. Moreover, nuclear accumulation of NFAT was drastically reduced in activated Gclc-deficient T cells compared to controls (Figure 5D), despite comparable Ca^{2+} mobilization (Figure S4E). Consequently, Gclc-deficient T cells secreted less IL-2, an NFAT target and T cell mitogen (Figure 5E). However, addition of IL-2 to *Cd4cre-Gclc^fl/fl* T cell cultures did not restore normal proliferation (Figure S4F), indicating that a lack of IL-2 is not the main factor blocking mutant T cell expansion. BSO reduced nuclear but not cytoplasmic NFAT in activated WT T cells (Figure 5F). Calcineurin normally dephosphorylates NFAT to allow its nuclear entry (Rusnak and Mertz, 2000). Calcineurin contains iron and zinc in its active site, and these are sensitive to high ROS (Namgaladze et al., 2002). We found that BSO-exposed WT T cells that we had treated with NAC to induce ROS scavenging easily initiated NFAT nuclear translocation (Figure 5F and Figure S4C). Accordingly, ROS buffering in Gclc-deficient T cells restored NFAT expression and nuclear translocation, as well as activation-induced IL-2 secretion (Figures 5G and 5H). Lastly, addition of NAC or GSH to *Cd4cre-Gclc^fl/fl* T cells increased expression of both Myc and its target CD98 in a manner sensitive to FK506 inhibition (Figure 5I). Thus, an antioxidative environment is needed for NFAT activation, Myc expression, and CD98 production in activated T cells. Our data show that ROS buffering by Gclc-derived GSH allows NFAT and mTOR to control the metabolic regulator Myc.

ROS Buffering Ensures the Integrity of T Cell Energy Metabolism

To investigate the impact of antioxidants on T cell metabolism, we activated *Cd4cre-Gclc^fl/fl* and control T cells in the presence of NAC or GSH and measured glucose consumption and lactate secretion. Gclc-deficient cells consumed less glucose and produced less lactate than controls, but they increased their

Figure 4. *Gclc* Mediates Metabolic Reprogramming and Glycolysis in Activated T Cells
(A) Luminescence determination of ATP in *Gclc^fl/fl* and *Cd4cre-Gclc^fl/fl* CD4$^+$ T cells that were stimulated with αCD3+αCD28 for 24 hr. Data are means ± SEM (n = 3) and representative of three independent trials.
(B) Extracellular acidification rates (ECAR) of Vβ8$^+$ CD4$^+$ and CD8$^+$ T cells that were isolated by cell sorting 48 hr after *Gclc^fl/fl* and *Cd4cre-Gclc^fl/fl* mice were injected with 150 μg SEB. Data are means ± SEM (n = 3) and representative of two independent trials.
(C) ECAR determination of *Gclc^fl/fl* and *Cd4cre-Gclc^fl/fl* CD4$^+$ and CD8$^+$ T cells that were stimulated with αCD3+αCD28 in vitro for 24 hr. Data are means ± SEM (n = 6) and representative of two independent trials.
(D and E) Extracellular glucose and lactate secretion rates (D), and the ratio of molecules of lactate produced per molecules of glucose consumed (E), in *Gclc^fl/fl* and *Cd4cre-Gclc^fl/fl* CD4$^+$ and CD8$^+$ cells that were stimulated with αCD3+αCD28 for 24 hr. Data are means ± SEM of triplicate measurements of pooled cells from four mice/genotype and are representative of three independent trials.
(F) Fluxmap of mammalian carbon metabolism (left) and mass isotopomer distribution of citrate (right) for *Gclc^fl/fl* and *Cd4cre-Gclc^fl/fl* CD4$^+$ T cells that were incubated with U-^{13}C-glucose and stimulated with αCD3+αCD28 for 24 hr. Data are means ± SEM (n = 3) and representative of three independent trials.
(G) Fractional carbon contribution of glucose, glutamine, and palmitate to citrate and malate in *Gclc^fl/fl* and *Cd4cre-Gclc^fl/fl* CD4$^+$ T cells that were stimulated with αCD3+αCD28 for 24 hr. Data are means ± SEM (n = 3) and representative of two independent trials.
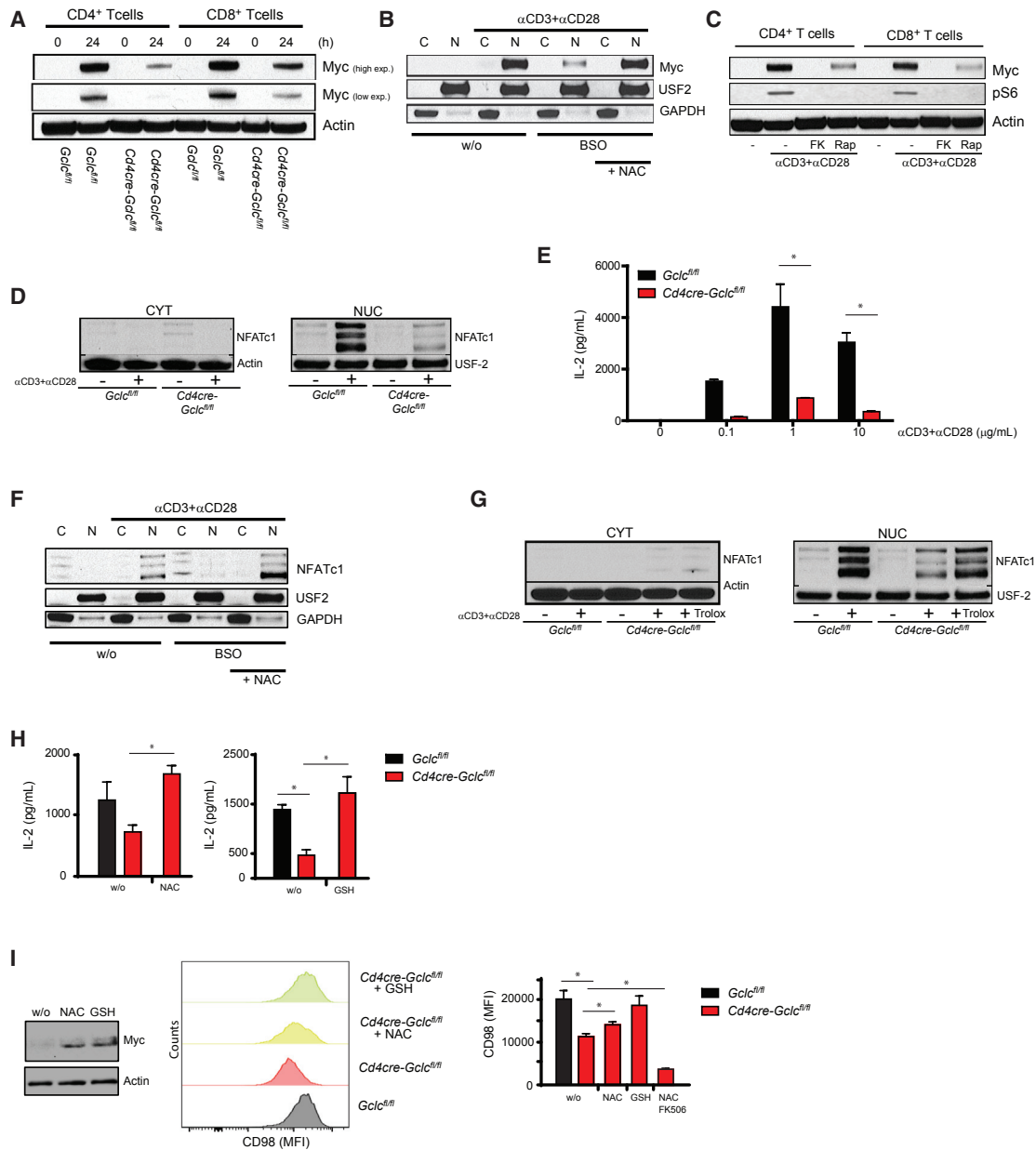
Figure 5. NFAT Activation and Myc Expression Rely on *Gclc*

(A) Immunoblot showing Myc expression in *Gclc^fl/fl^* and *Cd4cre-Gclc^fl/fl^* CD4⁺ and CD8⁺ T cells that were stimulated with αCD3+αCD28 for 24 hr. High and low exposures of one blot representative of four independent trials are shown.

(B) Immunoblot to detect Myc expression in cytosolic (C) and nuclear (N) subcellular fractions of the T cells stimulated as in (A) with or without BSO or NAC. USF2 and GAPDH, loading controls. Data are representative of two independent experiments.

(C) Immunoblot showing Myc expression in WT CD4⁺ and CD8⁺ T cells that were left untreated, or stimulated with αCD3+αCD28 for 24h and treated (or not) with FK506 (FK) or rapamycin (Rap). Data are representative of two independent trials.

(D) Immunoblot showing NFAT expression in cytoplasmic (CYT) and nuclear (NUC) fractions of *Gclc^fl/fl^* and *Cd4cre-Gclc^fl/fl^* CD4⁺ T cells that were stimulated with αCD3+αCD28 for 24 hr. Data are representative of four independent trials.

(E) ELISA of IL-2 secretion by *Gclc^fl/fl^* and *Cd4cre-Gclc^fl/fl^* CD4⁺ and CD8⁺ T cells that were stimulated with αCD3+αCD28 for 24 hr. Data are means ± SEM (n = 3) and representative of two independent trials.

(F) Immunoblot showing cytoplasmic and nuclear NFAT expression in T cells that were stimulated, fractionated, and analyzed as in (B). Data are representative of two independent experiments.

(G) Immunoblot showing cytoplasmic and nuclear NFAT expression in *Gclc^fl/fl^* and *Cd4cre-Gclc^fl/fl^* CD4⁺ T cells that were stimulated, fractionated, and analyzed for NFAT expression as in (D). T cells were also treated ± the ROS scavenger Trolox. Data are representative of four independent trials.

(legend continued on next page)

glycolytic activity in the presence of NAC or GSH (Figures 6A and 6B; see also Figures S5A and S5B). Measurement of glutamine flux into the TCA cycle via U-^{13}C-glutamine confirmed these findings (Figure 6C). We next assayed glucose and glutamine fluxes in activated WT T cells treated with BSO plus NAC or GSH. As was true for *Cd4cre-Gclc*$^{fl/fl}$ T cells, pharmacological inhibition of GCL in activated WT T cells reduced glucose and glutamine fluxes, which were restored by NAC or GSH (Figures S5C and S5D). Thus, GSH is critical for ROS buffering that allows metabolic reprogramming during T cell activation.

ROS scavenging in activated Gclc-deficient T cells also increased ATP and "recharged" these cells in a manner suppressed by FK506-mediated NFAT inhibition (Figure 6D). Antioxidant-treated "recharged" Gclc-deficient T cells mounted an activation-induced proliferative response and contained less ROS than untreated activated control T cells (Figure 6E and Figure S5E). BSO-treated WT T cells showed reduced proliferation that was restored by NAC (Figure 6F). As expected, the proliferation of NAC-treated activated *Cd4cre-Gclc*$^{fl/fl}$ T cells was inhibited by FK506 or rapamycin, indicating that proliferation in the presence of antioxidants is NFAT- and mTOR-dependent (Figures S5E and S5F).

One of our central hypotheses was that *Gclc*-controlled Myc was crucial for T cell functionality. We had already shown that both mTOR and NFAT control Myc in a manner influenced by antioxidants. To confirm that Myc is indeed affected by *Gclc* loss, we transduced *Cd4cre-Gclc*$^{fl/fl}$ T cells with a Myc-expressing retrovirus for 24 hr (Figure 6G). Surface expression of the Myc target CD98 was upregulated on Myc-expressing Gclc-deficient T cells compared to GFP-transduced controls (Figure 6G). Retroviral Myc expression also restored the proliferation of activated Gclc-deficient T cells (Figure 6H). Because the proliferation of Myc-expressing *Cd4cre-Gclc*$^{fl/fl}$ cells depends on NFAT, there must be a tight interaction between these pathways in T cells. We conclude that GSH preserves T cell metabolic integrity by supporting expression of Myc, which is closely linked to T cell functionality.

Ablation of *Gclc* in T Cells Leads to EAE Resistance in Mice

We next explored the consequences of the metabolic imbalance in Gclc-deficient T cells in vivo. Because *Gclc* activity affects T cell homeostasis, which is drastically disturbed in autoimmune diseases, we investigated whether targeting the GSH-dependent pathway might be a promising means of treating autoimmunity. Experimental autoimmune encephalomyelitis (EAE) is a mouse model of multiple sclerosis in which CD4$^+$ T cells are the major inflammatory drivers (Brüstle et al., 2007; Langrish et al., 2005). We induced EAE in age-matched *Gclc*$^{fl/fl}$ (control) and *Cd4cre-Gclc*$^{fl/fl}$ mice and immunized them subcutaneously (s.c.) with MOG peptide emulsion (MOG) plus pertussis toxin (PT) to induce disease (Brüstle et al., 2012). *Gclc*$^{fl/fl}$ mice developed severe EAE by day 30 (d30) post-induction, as expected,

whereas no *Cd4cre-Gclc*$^{fl/fl}$ mouse showed any signs of EAE during this period (Figure 7A). Histopathological analyses of brain tissue at d30 post-MOG immunization revealed immune cell infiltrates in control brains and spinal cords but not in those from *Cd4cre-Gclc*$^{fl/fl}$ mice (Figure 7B and Figure S6A). The infiltrates in the white matter of control (but not mutant) brains and spinal cords consisted mainly of CD3$^+$ T cells and activated macrophages or microglia (Figure 7B and Figure S6A). Because inflammatory T helper-17 (Th17) and Th1 cells are important for EAE (Brüstle et al., 2012), we analyzed these cells in control and *Cd4cre-Gclc*$^{fl/fl}$ mice at d12 post-EAE induction. *Cd4cre-Gclc*$^{fl/fl}$ CD4$^+$ T cells showed dramatically reduced IL-17 and IFN-γ secretion in comparison to controls (Figure 7C). Thus, *Gclc* is crucial for mounting an inflammatory T cell response in an autoimmune context.

Clearance of Acute Viral Infections Depends on *Gclc* Function in T Cells

The inability of *Cd4cre-Gclc*$^{fl/fl}$ mice to develop EAE suggested that they might lack a natural T cell-mediated defense against viral infections. We therefore measured T cell activation in vivo after a challenge with lymphocytic choriomeningitis virus (LCMV-Armstrong). We labeled CD8$^+$ T cells isolated from LCMV-specific (GP33 antigen) TCR transgenic (P14) *Gclc*$^{fl/fl}$ or *Cd4cre-Gclc*$^{fl/fl}$ mice with CFSE or violet cell trace (VCT), respectively, and transferred equal numbers of these cells into recipient mice. Activation of splenic T cells was measured at 36 and 60 hr post-LCMV infection of these recipients. In line with our in vivo results (Figure 1F), Gclc deficiency did not block the initial activation of LCMV-specific T cells in vivo (Figure 7D). However, when we infected *Cd4cre-Gclc*$^{fl/fl}$ and control mice with LCMV and monitored frequencies of antigen-specific CD8$^+$ T cells by tetramer staining (GP33, NP396) and flow cytometry, we found dramatic differences in the anti-viral response. In control mice, LCMV-reactive (GP33$^+$, NP396$^+$) T cells peaked at d8 post-infection, but only very low numbers of such T cells were detected in *Cd4cre-Gclc*$^{fl/fl}$ mice (Figure 7E), and very few of these produced inflammatory cytokines (Figure 7F). Accordingly, whereas control mice cleared the virus by d8 post-infection, viral titers remained high in the mutants (Figure 7G). At d60 post-infection, LCMV-specific memory CD8$^+$ T cells (CD44^{high}, CD62L^{high}, CD127^{high}, KLRG1^{low}) and cytokine-producing cells were still drastically reduced in *Cd4cre-Gclc*$^{fl/fl}$ mice compared to controls (Figure 7H and Figure S6B). In contrast, activation of the innate immune system was not obviously affected by T cell loss of *Gclc*; equivalent secretion of type I IFN was detected in the serum of control and mutant mice on d3 post-infection (Figure S6C).

Our earlier data showed that *Cd4cre-Gclc*$^{fl/fl}$ mice have fewer T cells (Figure S1F). To rule out the possibility that this altered T cell homeostasis affected the response of *Cd4cre-Gclc*$^{fl/fl}$ mice to LCMV, we adoptively transferred P14-specific, VCT-labeled *Cd4cre-Gclc*$^{fl/fl}$ CD8$^+$ T cells and P14-specific,

---

(H) ELISA of IL-2 secretion by *Gclc*$^{fl/fl}$ and *Cd4cre-Gclc*$^{fl/fl}$ CD4$^+$ T cells that were stimulated for 24 hr with αCD3+αCD28 and with or without (w/o) NAC or GSH. Data are means ± SEM (n = 3) and representative of two independent trials.

(I) Left: Immunoblot showing Myc accumulation in *Gclc*$^{fl/fl}$ and *Cd4cre-Gclc*$^{fl/fl}$ CD4$^+$ T cells that were stimulated and treated as in (H). Middle and right: Flow-cytometric analysis of CD98 surface expression. Data on the right are means ± SEM (n = 3). Results are representative of three independent trials. See also Figure S4.
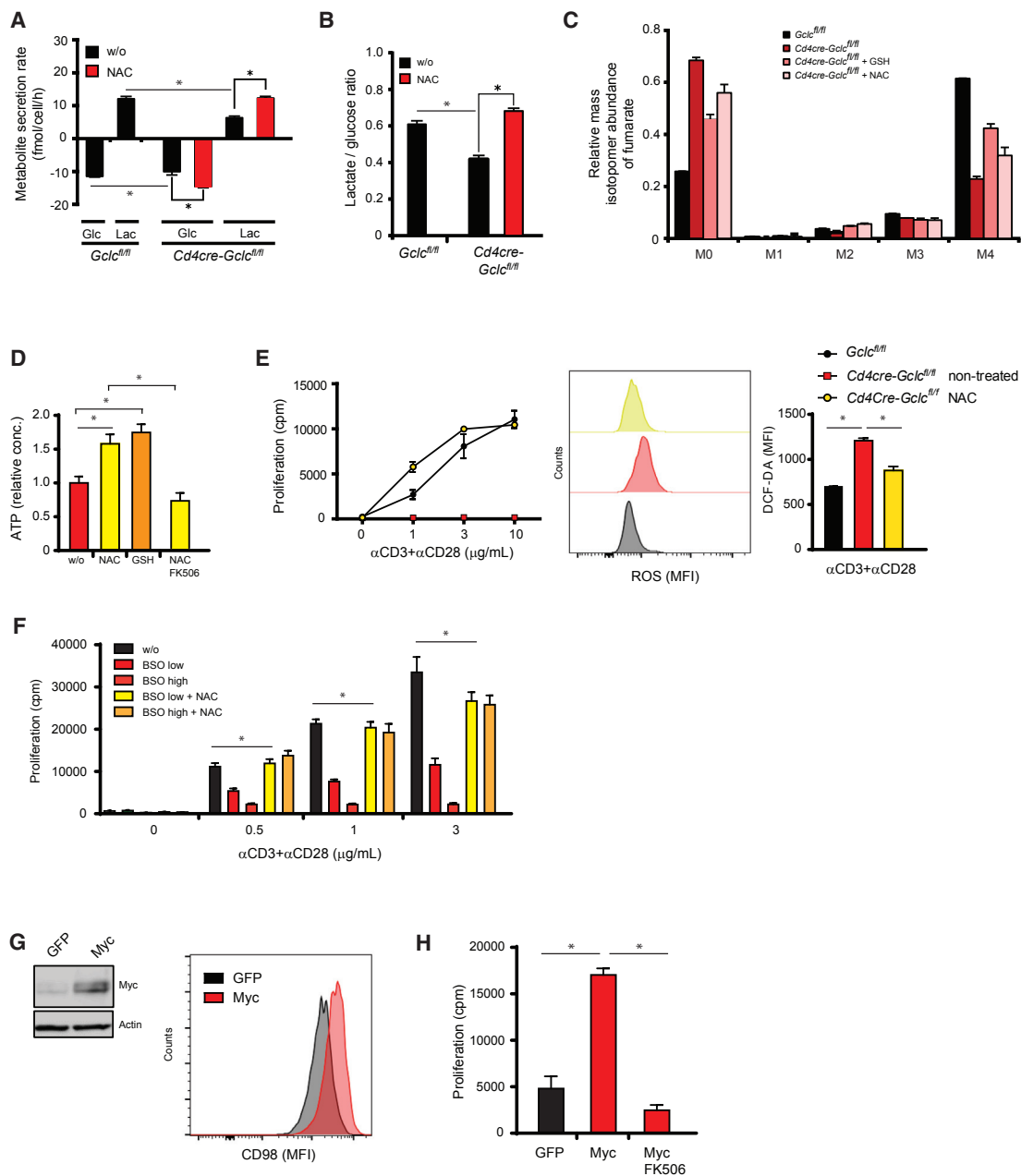
Figure 6. T-Cell-Intrinsic *Gclc* Controls the Integrity of T Cell Metabolism in a Myc-Dependent Manner

(A and B) Measurement of glucose and lactate secretion rates (A), and the ratio of molecules of lactate produced per molecules of glucose consumed (B), in *Gclc^fl/fl* and *Cd4cre-Gclc^fl/fl* CD4^{+} T cells that were stimulated with αCD3+αCD28 for 24 hr ± NAC. Data are means ± SEM of triplicate measurements of pooled cells from four mice/genotype and representative of three independent trials.

(C) Mass isotopomer distribution of fumarate for *Gclc^fl/fl* and *Cd4cre-Gclc^fl/fl* CD4^{+} T cells that were incubated with U-^{13}C-glutamine and stimulated with αCD3+αCD28 for 24 hr ± NAC or GSH. Data are means ± SEM (n = 3) and representative of three independent trials.

(D) Determination of intracellular ATP concentrations in *Gclc^fl/fl* and *Cd4cre-Gclc^fl/fl* T cells that were stimulated for 24 hr with αCD3+αCD28 alone (w/o) or ± NAC, GSH, or NAC+FK506. Data are means ± SEM (n = 3) and representative of two independent trials.

(E) Left: Proliferation assessment by ^{3}H-thymidine incorporation of *Gclc^fl/fl* and *Cd4cre-Gclc^fl/fl* T cells that were stimulated with αCD3+αCD28 for 24 hr ± NAC. Middle, right: ROS concentrations were assessed by DCF-DA staining and flow cytometry. Data are means ± SEM (n = 3) and representative of three independent trials.

(F) Proliferation assessment by ^{3}H-thymidine incorporation of WT T cells that were treated ± BSO (low, 200 μM; high, 1,000 μM) and stimulated with αCD3+αCD28 for 24 hr ± NAC. Data are means ± SEM (n = 3) and representative of two independent trials.

(legend continued on next page)

CFSE-labeled CD8^{+} T cells into recipient mice and infected these animals with LCMV. Although the transferred cells were antigen-specific (P14) and showed a similar degree of T cell activation (Figure 7D), P14-*Cd4cre-Gclc^{fl/fl}* mice did not mount an anti-viral proliferative response (Figure S6D). Thus, intrinsic *Gclc* expression in T cells is required for antigen-specific anti-viral immunity.

DISCUSSION

Although moderate concentrations of ROS act as signaling messengers and modify protein function or structure by oxidation, high concentrations of ROS lead to cell death, mutagenesis, or tumorigenesis (Gorrini et al., 2013; Harris et al., 2015; Sena and Chandel, 2012). TCR stimulation induces mitochondrial ROS production that influences T cell activation, proliferation, and effector functions (Devadas et al., 2002; Gülow et al., 2005; Jackson et al., 2004; Sena et al., 2013; Yi et al., 2006). Prevention of lipid oxidation by glutathione peroxidase 4 (Gpx4) is crucial for T cell survival and activation (Matsushita et al., 2015). However, prior to our study, the importance of GCL function in T cells was unclear. By targeting *Gclc* in T cells, we have demonstrated that antioxidation by GSH supports an environment essential for activation-induced metabolic reprogramming in T cells.

Cd4cre-Gclc^{fl/fl} T cells did not proliferate upon TCR ligation, and mTORC1 activation was impaired. These findings are in line with mTOR's regulation of cell growth, which is controlled by a glutamine flux dependent on CD98 upregulation (Nakaya et al., 2014; Nicklin et al., 2009; Sinclair et al., 2013). Glutamine enters the TCA cycle as αKG. However, addition of glutamine or DMK to cultures of Gclc-deficient T cells did not rescue their metabolic deficit, indicating that GSH might be a master regulator of metabolism in this cell type and is not limited to controlling mTORC1 or glutaminolysis. Indeed, GSH is critical for Myc expression in activated T cells, and Myc is linked to the glutaminolysis and glycolysis characteristic of metabolic reprogramming (Verbist et al., 2016; Wang et al., 2011). Gclc-deficient T cells accumulate moderate concentrations of ROS, which can inhibit phosphatases via oxidation of their catalytic residues (Kamata et al., 2005; McCubrey et al., 2006) and can block the phosphatase-sensitive MAPK- and NFAT-involving pathways that drive Myc expression (Buchholz et al., 2006; Köenig et al., 2010; Singh et al., 2010). Calcineurin dephosphorylates NFAT in the cytosol, initiating NFAT nuclear translocation (Rusnak and Mertz, 2000). Technical reasons prevented us from demonstrating inactivity of calcineurin under conditions involving high concentrations of ROS, but we did show that BSO treatment of activated WT cells decreased NFAT nuclear translocation and led to the accumulation of NFAT in the cytoplasm. This reduction in NFAT activity suppressed Myc and CD98 expression and was directly linked to elevated concentrations of ROS. Consequently, *Cd4cre-Gclc^{fl/fl}* T cells displayed dramatically reduced Myc, did not shift their metabolism to glycolysis and glutaminolysis, and instead utilized fatty-acid β-oxidation. Proliferation and functionality of Gclc-deficient T cells was restored by retroviral Myc expression, identifying Myc as the central effector in this pathway.

Our data further imply that T cell activation imposes a metabolic burden that slowly depletes the energy pool of Gclc-deficient T cells, as confirmed by their decreased ATP. Low ATP abundance can interfere with the mTOR pathway (Hardie et al., 2012), in line with the reduced mTOR activation in *Cd4cre-Gclc^{fl/fl}* T cells. Notably, there is a ying-yang relationship between mTOR and Myc. Myc represses transcription of TSC2, increasing mTOR activity (Schmidt et al., 2009), but mTOR phosphorylates 4E-BP1 and releases the translation initiation factor eIF-4e, which drives Myc translation (West et al., 1998). Thus, the low Myc expression in Gclc-deficient T cells might negatively affect mTOR activation and vice versa. Alternatively, AKT, which is regulated by PI3K and PTEN (Laplante and Sabatini, 2012), can suppress mTOR activity (Hahn-Windgassen et al., 2005; Inoki et al., 2002). However, AKT activation was not altered by the loss of Gclc in T cells.

Gclc-deficient T cells underwent normal early activation in vitro and in vivo but were unable to proliferate. Increased glucose metabolism is important for proliferation, but mitochondrial respiration prior to proliferation is sufficient for T cell activation (Sena et al., 2013). High concentrations of ROS are known to inhibit glyceraldehyde-3-phosphatase dehydrogenase and thereby impede glycolysis (Hwang et al., 2009). During early proliferation (24 hr after TCR ligation), activated T cells require fatty acids for lipid and membrane synthesis. These components are provided by metabolic reprogramming that increases acetyl-CoA synthesis from glucose and glutamine and fuels the cellular energy pool (Pearce and Pearce, 2013). Without *Gclc* and thus GSH, this process is disturbed, and the fatty-acid oxidation required for driving energy production and cell growth represents a severe metabolic burden to the T cell. If GSH-deficient T cells cannot compensate for their ongoing deficit in acetyl-CoA by using either glucose or glutamine as a carbon source, they eventually succumb to cell death. In vivo, T cell-specific ablation of the GSH pathway manifests as dysregulated autoimmune responses and impaired antiviral defense. Our results demonstrate that the GSH antioxidative system tightly links the metabolic reprogramming in activated T cells to the regulation of immune homeostasis.

EXPERIMENTAL PROCEDURES

Mice

T Cell Isolation, Activation, and Proliferation

CD4^{+} and CD8^{+} T cells were isolated from spleen and LNs by magnetic bead sorting (Miltenyi). T cells were stimulated in vitro with PMA (Sigma, 200 ng/mL) and calcium ionophore A23187 (Iono; Sigma, 200 ng/mL), with anti-CD3 antibody (BD Biosciences, 4 μg/mL) plus anti-CD28 antibody (BD Biosciences,

---

(G) *Cd4cre-Gclc^{fl/fl}* T cells were stimulated with αCD3+αCD28 and infected with control or Myc-expressing retrovirus. T cells were sorted by flow cytometry and reactivated in vitro with αCD3+αCD28 for 24 hr. Left: Immunoblot showing Myc accumulation. Right: Flow-cytometric determination of CD98 surface expression. Data are representative of three independent trials.

(H) Proliferation assessment by ^{3}H-thymidine incorporation of *Cd4cre-Gclc^{fl/fl}* T cells that were infected and sorted as in (G). Data are means ± SEM (n = 3) and representative of three independent trials. See also Figure S5.
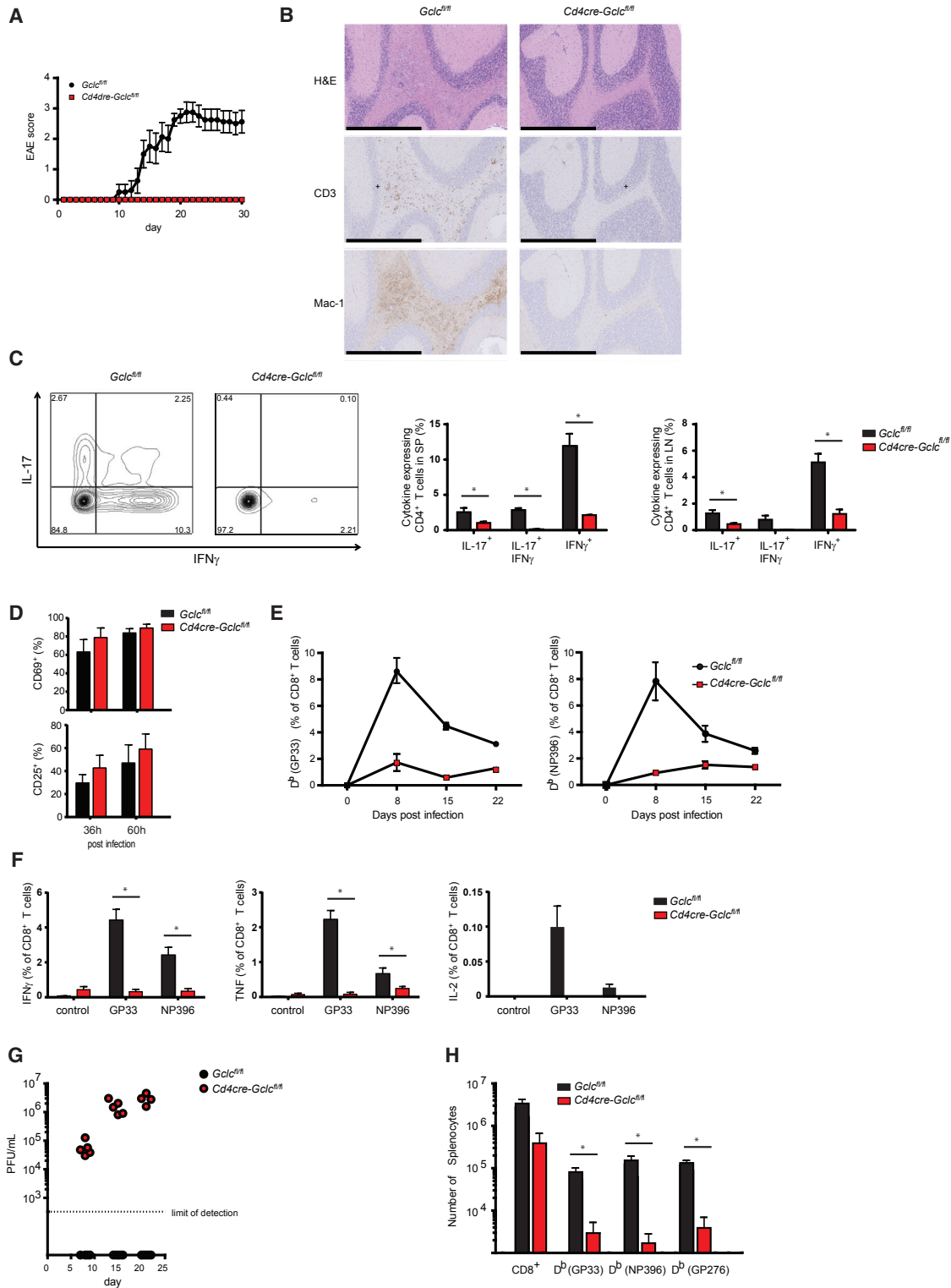
Figure 7. Autoimmune and Anti-viral Responses Depend on *Gclc* in T Cells

(A) EAE induction time course in *Gclc*$^{fl/fl}$ (n = 8) and *Cd4cre-Gclc*$^{fl/fl}$ (n = 8) mice that were immunized with MOG peptide. Data are means ± SEM and representative of two independent trials.

(B) Histological analyses of brains of the mice in (A) on d30 post-EAE induction. Cross-sections of the same brain area were stained with H&E, anti-CD3 antibody (for detection of T cells), or anti-Mac-1 antibody (macrophages, activated microglia). Scale bars represent 400 μm. Results are for one mouse/genotype representative of three mice/group. Data are representative of two independent trials.

(legend continued on next page)

2 μg/mL), or with MOG peptide for the times or at the concentrations indicated in the Figures.

In Vivo T Cell Activation

Mice were injected intraperitoneally (i.p.) with 150 μg/mouse Staphylococcal enterotoxin B (Sigma). After 48 hr, T cells were analyzed for ROS as described in the main text, analyzed for GSH amounts as described below, or sorted by standard flow cytometry so that Vβ8+ T cells could be isolated. Alternatively, mice were injected i.p. with 50 μg/anti-CD3 (Biolegend). After 24 hr, T cells were analyzed for ROS as described in the main text or analyzed for GSH amounts as described below.

Proliferation

For assessment of cell proliferation, ^{3}H-thymidine incorporation was measured with a Matrix 96 Direct β Counter (Canberra Packard) 24 hr after stimulation, as described previously (Brenner et al., 2014).

EAE Induction

Mice were injected s.c. with MOG 35-55 peptide (Washington Biotech) plus CFA (Difco) emulsion, followed by two intraperitoneal injections of pertussis toxin (PT, List Biological), as described (Brüstle et al., 2012). Clinical scores were determined as described (Brüstle et al., 2012). Brains and spinal cords were obtained 30 days after EAE induction, and histological sections were analyzed as described (Brenner et al., 2014; Brüstle et al., 2012).

LCMV Infection

Mice were infected i.p. with 5 × 10^5 PFU LCMV-Armstrong. LCMV-specific T cells were identified in peripheral blood or spleen via staining with GP33-, NP396-, or GP276-specific tetramers (National Institutes of Health) followed by flow cytometry. Virus titers were determined by plaque-forming assays as described (Ahmed et al., 1984).

Intracellular ROS

T cells were stimulated with PMA (10 ng/mL) plus Iono (10 ng/mL) or with anti-CD3 plus anti-CD28 antibodies (1μg), for 24 hr before 30 min incubation with 5 μM dichlorofluorescein diacetate (DCF-DA, Sigma). Cells were analyzed by flow cytometry as described (Gülow et al., 2005).

Isotopic Labeling

T cells were incubated for 24 hr in RPMI 1640 containing [U-^{13}C]-glucose (11.1 mmol/L; Cambridge Isotope Laboratories); [U-^{13}C]-glutamine (2 mmol/L; Cambridge Isotope Laboratories); or [U-^{13}C]-palmitate (0.1 mmol/L, Sigma) conjugated to bovine serum albumin (Sigma). Extraction of intracellular metabolites, GC-MS measurement, and calculation of mass isotopomer distributions and fractional carbon contributions were performed as described (Battello et al., 2016). Glucose, lactate, glutamine, and glutamate concentrations were determined with a YSI 2950D Biochemistry Analyzer (YSI Incorporated).

Statistics

Data are means ± SEM, and p values were determined by unpaired Student's t test or two-way Anova test with Prism 7.0 (GraphPad). p values ≤ 0.05 were considered significant.

Study Approval

Animal procedures were approved by the University Health Network Institutional Animal Care and Use Committee in Toronto and/or the Animal Welfare Structure at the Luxembourg Institute of Health.

REFERENCES

Ahmed, R., Salmi, A., Butler, L.D., Chiller, J.M., and Oldstone, M.B. (1984). Selection of genetic variants of lymphocytic choriomeningitis virus in spleens of persistently infected mice. Role in suppression of cytotoxic T lymphocyte response and viral persistence. J. Exp. Med. 160, 521–540.

Babcock, J.T., Nguyen, H.B., He, Y., Hendricks, J.W., Wek, R.C., and Quilliam, L.A. (2013). Mammalian target of rapamycin complex 1 (mTORC1) enhances bortezomib-induced death in tuberous sclerosis complex (TSC)-null cells

(C) Intracellular staining and flow cytometry showing IL-17 and IFN-γ in CD4+ T cells from spleen (left, middle) and LN (right) of *Gclc$^{fl/fl}$* and *Cd4cre-Gclc$^{fl/fl}$* mice at d12 post-EAE induction. Left: Data are gated on live CD4+ T cells. Middle, right: Data are means ± SEM (n = 4) and representative of three independent trials.

(D) CD8+ T cells from LCMV-specific TCR transgenic *P14-Gclc$^{fl/fl}$* (n = 6) and *P14-Cd4cre-Gclc$^{fl/fl}$* (n = 6) mice were isolated from spleen and LNs, labeled with CFSE or VCT, respectively, and transferred into WT recipient mice. Recipients were infected with LCMV-Armstrong. At the indicated times after infection, splenic T cells were isolated from recipients and analyzed for CD69 and CD25 surface expression by flow cytometry. Data are means ± SEM (n = 4) and representative of two independent trials.

(E) Flow-cytometric determination of LCMV-reactive T cells in *Gclc$^{fl/fl}$* (n = 12) and *Cd4cre-Gclc$^{fl/fl}$* (n = 12) mice that were infected with LCMV-Armstrong. T cells were stained with tetramers specific for the LCMV peptides GP33 (left) and NP396 (right) and evaluated at the indicated times. Data are means ± SEM and representative of two independent trials.

(F) Intracellular flow-cytometric determination of expression of the indicated cytokines by splenic LCMV-specific CD8+ T cells measured at d8 post-infection. Data are means ± SEM (n = 4/genotype) and representative of two independent trials.

(G) Viral titers in the mice in (E) were determined at the indicated times via plaque-forming assays. Data are means ± SEM (n = 5/genotype).

(H) Flow-cytometric quantitation of antigen-specific memory T cells at d60 post-LCMV infection. Data are means ± SEM (n = 6/genotype) and representative of two independent trials. See also Figure S6.

by a c-MYC-dependent induction of the unfolded protein response. J. Biol. Chem. *288*, 15687–15698.

Battello, N., Zimmer, A.D., Goebel, C., Dong, X., Behrmann, I., Haan, C., Hiller, K., and Wegner, A. (2016). The role of HIF-1 in oncostatin M-dependent metabolic reprogramming of hepatic cells. Cancer Metab. *4*, 3.

Brenner, D., Brüstle, A., Lin, G.H., Lang, P.A., Duncan, G.S., Knobbe-Thomsen, C.B., St Paul, M., Reardon, C., Tusche, M.W., Snow, B., et al. (2014). Toso controls encephalitogenic immune responses by dendritic cells and regulatory T cells. Proc. Natl. Acad. Sci. USA *111*, 1060–1065.

Brownlie, R.J., and Zamoyska, R. (2013). T cell receptor signalling networks: branched, diversified and bounded. Nat. Rev. Immunol. *13*, 257–269.

Brüstle, A., Heink, S., Huber, M., Rosenplänter, C., Stadelmann, C., Yu, P., Arpaia, E., Mak, T.W., Kamradt, T., and Lohoff, M. (2007). The development of inflammatory T(H)-17 cells requires interferon-regulatory factor 4. Nat. Immunol. *8*, 958–966.

Brüstle, A., Brenner, D., Knobbe, C.B., Lang, P.A., Virtanen, C., Hershenfield, B.M., Reardon, C., Lacher, S.M., Ruland, J., Ohashi, P.S., and Mak, T.W. (2012). The NF-κB regulator MALT1 determines the encephalitogenic potential of Th17 cells. J. Clin. Invest. *122*, 4698–4709.

Buchholz, M., Schatz, A., Wagner, M., Michl, P., Linhart, T., Adler, G., Gress, T.M., and Ellenrieder, V. (2006). Overexpression of c-myc in pancreatic cancer caused by ectopic activation of NFATc1 and the Ca2+/calcineurin signaling pathway. EMBO J. *25*, 3714–3724.

Cairns, R.A., Harris, I.S., and Mak, T.W. (2011). Regulation of cancer cell metabolism. Nat. Rev. Cancer *11*, 85–95.

Carr, E.L., Kelman, A., Wu, G.S., Gopaul, R., Senkevitch, E., Aghvanyan, A., Turay, A.M., and Frauwirth, K.A. (2010). Glutamine uptake and metabolism are coordinately regulated by ERK/MAPK during T lymphocyte activation. J. Immunol. *185*, 1037–1044.

Chang, C.H., Curtis, J.D., Maggi, L.B., Jr., Faubert, B., Villarino, A.V., O'Sullivan, D., Huang, S.C., van der Windt, G.J., Blagih, J., Qiu, J., et al. (2013). Posttranscriptional control of T cell effector function by aerobic glycolysis. Cell *153*, 1239–1251.

Chen, Y., Shertzer, H.G., Schneider, S.N., Nebert, D.W., and Dalton, T.P. (2005). Glutamate cysteine ligase catalysis: dependence on ATP and modifier subunit for regulation of tissue glutathione levels. J. Biol. Chem. *280*, 33766–33774.

Chen, Y., Yang, Y., Miller, M.L., Shen, D., Shertzer, H.G., Stringer, K.F., Wang, B., Schneider, S.N., Nebert, D.W., and Dalton, T.P. (2007). Hepatocyte-specific Gclc deletion leads to rapid onset of steatosis with mitochondrial injury and liver failure. Hepatology *45*, 1118–1128.

David, C.J., Chen, M., Assanah, M., Canoll, P., and Manley, J.L. (2010). HnRNP proteins controlled by c-Myc deregulate pyruvate kinase mRNA splicing in cancer. Nature *463*, 364–368.

Devadas, S., Zaritskaya, L., Rhee, S.G., Oberley, L., and Williams, M.S. (2002). Discrete generation of superoxide and hydrogen peroxide by T cell receptor stimulation: selective regulation of mitogen-activated protein kinase activation and fas ligand expression. J. Exp. Med. *195*, 59–70.

Douglas, N.C., Jacobs, H., Bothwell, A.L., and Hayday, A.C. (2001). Defining the specific physiological requirements for c-Myc in T cell development. Nat. Immunol. *2*, 307–315.

Düvel, K., Yecies, J.L., Menon, S., Raman, P., Lipovsky, A.I., Souza, A.L., Triantafellow, E., Ma, Q., Gorski, R., Cleaver, S., et al. (2010). Activation of a metabolic gene regulatory network downstream of mTOR complex 1. Mol. Cell *39*, 171–183.

Frauwirth, K.A., Riley, J.L., Harris, M.H., Parry, R.V., Rathmell, J.C., Plas, D.R., Elstrom, R.L., June, C.H., and Thompson, C.B. (2002). The CD28 signaling pathway regulates glucose metabolism. Immunity *16*, 769–777.

Gerriets, V.A., and Rathmell, J.C. (2012). Metabolic pathways in T cell fate and function. Trends Immunol. *33*, 168–173.

Gorrini, C., Harris, I.S., and Mak, T.W. (2013). Modulation of oxidative stress as an anticancer strategy. Nat. Rev. Drug Discov. *12*, 931–947.

Gülow, K., Kaminski, M., Darvas, K., Süss, D., Li-Weber, M., and Krammer, P.H. (2005). HIV-1 trans-activator of transcription substitutes for oxidative signaling in activation-induced T cell death. J. Immunol. *174*, 5249–5260.

Hahn-Windgassen, A., Nogueira, V., Chen, C.C., Skeen, J.E., Sonenberg, N., and Hay, N. (2005). Akt activates the mammalian target of rapamycin by regulating cellular ATP level and AMPK activity. J. Biol. Chem. *280*, 32081–32089.

Hardie, D.G., Ross, F.A., and Hawley, S.A. (2012). AMPK: a nutrient and energy sensor that maintains energy homeostasis. Nat. Rev. Mol. Cell Biol. *13*, 251–262.

Harris, I.S., Treloar, A.E., Inoue, S., Sasaki, M., Gorrini, C., Lee, K.C., Yung, K.Y., Brenner, D., Knobbe-Thomsen, C.B., Cox, M.A., et al. (2015). Glutathione and thioredoxin antioxidant pathways synergize to drive cancer initiation and progression. Cancer Cell *27*, 211–222.

Hörig, H., Spagnoli, G.C., Filgueira, L., Babst, R., Gallati, H., Harder, F., Juretic, A., and Heberer, M. (1993). Exogenous glutamine requirement is confined to late events of T cell activation. J. Cell. Biochem. *53*, 343–351.

Hosoi, H., Dilling, M.B., Liu, L.N., Danks, M.K., Shikata, T., Sekulic, A., Abraham, R.T., Lawrence, J.C., Jr., and Houghton, P.J. (1998). Studies on the mechanism of resistance to rapamycin in human cancer cells. Mol. Pharmacol. *54*, 815–824.

Hwang, N.R., Yim, S.H., Kim, Y.M., Jeong, J., Song, E.J., Lee, Y., Lee, J.H., Choi, S., and Lee, K.J. (2009). Oxidative modifications of glyceraldehyde-3-phosphate dehydrogenase play a key role in its multiple cellular functions. Biochem. J. *423*, 253–264.

Inoki, K., Li, Y., Zhu, T., Wu, J., and Guan, K.L. (2002). TSC2 is phosphorylated and inhibited by Akt and suppresses mTOR signalling. Nat. Cell Biol. *4*, 648–657.

Inoki, K., Ouyang, H., Zhu, T., Lindvall, C., Wang, Y., Zhang, X., Yang, Q., Bennett, C., Harada, Y., Stankunas, K., et al. (2006). TSC2 integrates Wnt and energy signals via a coordinated phosphorylation by AMPK and GSK3 to regulate cell growth. Cell *126*, 955–968.

Jackson, S.H., Devadas, S., Kwon, J., Pinto, L.A., and Williams, M.S. (2004). T cells express a phagocyte-type NADPH oxidase that is activated after T cell receptor stimulation. Nat. Immunol. *5*, 818–827.

Kamata, H., Honda, S., Maeda, S., Chang, L., Hirata, H., and Karin, M. (2005). Reactive oxygen species promote TNFalpha-induced death and sustained JNK activation by inhibiting MAP kinase phosphatases. Cell *120*, 649–661.

Köenig, A., Linhart, T., Schlengemann, K., Reutlinger, K., Wegele, J., Adler, G., Singh, G., Hofmann, L., Kunsch, S., Büch, T., et al. (2010). NFAT-induced histone acetylation relay switch promotes c-Myc-dependent growth in pancreatic cancer cells. Gastroenterology *138*, 1189–99.e1, 2.

Langrish, C.L., Chen, Y., Blumenschein, W.M., Mattson, J., Basham, B., Sedgwick, J.D., McClanahan, T., Kastelein, R.A., and Cua, D.J. (2005). IL-23 drives a pathogenic T cell population that induces autoimmune inflammation. J. Exp. Med. *201*, 233–240.

Laplante, M., and Sabatini, D.M. (2012). mTOR signaling in growth control and disease. Cell *149*, 274–293.

Matsushita, M., Freigang, S., Schneider, C., Conrad, M., Bornkamm, G.W., and Kopf, M. (2015). T cell lipid peroxidation induces ferroptosis and prevents immunity to infection. J. Exp. Med. *212*, 555–568.

McCubrey, J.A., Lahair, M.M., and Franklin, R.A. (2006). Reactive oxygen species-induced activation of the MAP kinase signaling pathways. Antioxid. Redox Signal. *8*, 1775–1789.

Meister, A. (1983). Selective modification of glutathione metabolism. Science *220*, 472–477.

Nakaya, M., Xiao, Y., Zhou, X., Chang, J.H., Chang, M., Cheng, X., Blonska, M., Lin, X., and Sun, S.C. (2014). Inflammatory T cell responses rely on amino acid transporter ASCT2 facilitation of glutamine uptake and mTORC1 kinase activation. Immunity *40*, 692–705.

Namgaladze, D., Hofer, H.W., and Ullrich, V. (2002). Redox control of calcineurin by targeting the binuclear Fe(2+)-Zn(2+) center at the enzyme active site. J. Biol. Chem. *277*, 5962–5969.

Newsholme, E.A., Crabtree, B., and Ardawi, M.S. (1985). Glutamine metabolism in lymphocytes: Its biochemical, physiological and clinical importance. Q. J. Exp. Physiol. 70, 473–489.

Nicklin, P., Bergman, P., Zhang, B., Triantafellow, E., Wang, H., Nyfeler, B., Yang, H., Hild, M., Kung, C., Wilson, C., et al. (2009). Bidirectional transport of amino acids regulates mTOR and autophagy. Cell 136, 521–534.

Pearce, E.L., and Pearce, E.J. (2013). Metabolic pathways in immune cell activation and quiescence. Immunity 38, 633–643.

Pollizzi, K.N., and Powell, J.D. (2014). Integrating canonical and metabolic signalling programmes in the regulation of T cell responses. Nat. Rev. Immunol. 14, 435–446.

Rusnak, F., and Mertz, P. (2000). Calcineurin: form and function. Physiol. Rev. 80, 1483–1521.

Schmidt, E.V., Ravitz, M.J., Chen, L., and Lynch, M. (2009). Growth controls connect: interactions between c-myc and the tuberous sclerosis complex-mTOR pathway. Cell Cycle 8, 1344–1351.

Sena, L.A., and Chandel, N.S. (2012). Physiological roles of mitochondrial reactive oxygen species. Mol. Cell 48, 158–167.

Sena, L.A., Li, S., Jairaman, A., Prakriya, M., Ezponda, T., Hildeman, D.A., Wang, C.R., Schumacker, P.T., Licht, J.D., Perlman, H., et al. (2013). Mitochondria are required for antigen-specific T cell activation through reactive oxygen species signaling. Immunity 38, 225–236.

Sinclair, L.V., Rolf, J., Emslie, E., Shi, Y.B., Taylor, P.M., and Cantrell, D.A. (2013). Control of amino-acid transport by antigen receptors coordinates the metabolic reprogramming essential for T cell differentiation. Nat. Immunol. 14, 500–508.

Singh, G., Singh, S.K., König, A., Reutlinger, K., Nye, M.D., Adhikary, T., Eilers, M., Gress, T.M., Fernandez-Zapico, M.E., and Ellenrieder, V. (2010). Sequential activation of NFAT and c-Myc transcription factors mediates the TGF-beta switch from a suppressor to a promoter of cancer cell proliferation. J. Biol. Chem. 285, 27241–27250.

Verbist, K.C., Guy, C.S., Milasta, S., Liedmann, S., Kamiński, M.M., Wang, R., and Green, D.R. (2016). Metabolic maintenance of cell asymmetry following division in activated T lymphocytes. Nature 532, 389–393.

Wang, R., Dillon, C.P., Shi, L.Z., Milasta, S., Carter, R., Finkelstein, D., McCormick, L.L., Fitzgerald, P., Chi, H., Munger, J., and Green, D.R. (2011). The transcription factor Myc controls metabolic reprogramming upon T lymphocyte activation. Immunity 35, 871–882.

West, M.J., Stoneley, M., and Willis, A.E. (1998). Translational induction of the c-myc oncogene via activation of the FRAP/TOR signalling pathway. Oncogene 17, 769–780.

Wolfer, A., Bakker, T., Wilson, A., Nicolas, M., Ioannidis, V., Littman, D.R., Lee, P.P., Wilson, C.B., Held, W., MacDonald, H.R., and Radtke, F. (2001). Inactivation of Notch 1 in immature thymocytes does not perturb CD4 or CD8T cell development. Nat. Immunol. 2, 235–241.

Yaqoob, P., and Calder, P.C. (1997). Glutamine requirement of proliferating T lymphocytes. Nutrition 13, 646–651.

Yi, J.S., Holbrook, B.C., Michalek, R.D., Laniewski, N.G., and Grayson, J.M. (2006). Electron transport complex I is required for CD8+ T cell function. J. Immunol. 177, 852–862.